

Joint Optimal Scheduling for Electric Vehicle Battery Swapping-charging Systems Based on Wind Farms

Mingfei Ban[✉], Member, IEEE, Jilai Yu, and Yiyun Yao, Member, IEEE

Abstract—Insufficiencies in charging facilities limit the broad application of electric vehicles (EVs). In addition, EV can hardly represent a green option if its electricity primarily depends on fossil energy. Considering these two problems, this paper studies a battery swapping-charging system based on wind farms (hereinafter referred to as W-BSCS). In a W-BSCS, the wind farms not only supply electricity to the power grid but also cooperate with a centralized charge station (CCS), which can centrally charge EV batteries and then distribute them to multiple battery swapping stations (BSSs). The operational framework of the W-BSCS is analyzed, and some preprocessing technologies are developed to reduce complexity in modeling. Then, a joint optimal scheduling model involving a wind power generation plan, battery swapping demand, battery charging and discharging, and a vehicle routing problem (VRP) is established. Then a heuristic method based on the exhaustive search and the Genetic Algorithm is employed to solve the formulated NP-hard problem. Numerical results verify the effectiveness of the joint optimal scheduling model, and they also show that the W-BSCS has great potential to promote EVs and wind power.

Index Terms—Battery swapping station, electric vehicle, vehicle routing problem, wind power.

NOMENCLATURE

A. Sets and Indices

k/K	Index/set of battery transporter (BTs).
$m(n)/B$	Index/set of battery swapping stations (BSSs).
t/T	Index/set for scheduling periods.
$r_{k,t}/P_k$	Index/set for battery supplement stations (W-CCS ^R).

B. Parameters

C_{total}	Total cost [\$].
C_{plan}	Penalty for failing to complete generation plan [\$].

C_{BSS}	Penalty for failing to fulfill demand of BSSs [\$].
C_{delivery}	Routing cost for the battery delivery vehicles [\$].
C_{grid}	Cost for buying electricity from power grid [\$].
C_{wind}	Penalty for wind curtailment of the W-CCS [\$].
γ_t^{plan}	Price for failing to complete generation plan [\$/MWh].
$\gamma_m^{\text{BSS}^*}$	Price for failing to fulfill demand of BSSs [\$/MWh].
$\gamma_k^{m,n}$	Price for BT _k travel cost between vertices m and n [\$].
$\gamma_t^{\text{grid}^*}$	Price for buying electricity from power grid [\$/MWh].
$\gamma_t^{\text{wind}^*}$	Penalty for wind curtailment of the W-CCS [\$/MWh].
N_{max}	Upper limits for the visit times of BTs to a BSS.
$d^{m,n}$	Driving distance between m and n [km].
D_k^{max}	Upper limit for driving distance of BT _k [km].
$\Delta\tau_k^{m,n}$	Travel time of BT _k between vertices m and n [Δt].
$\underline{\tau}^m$	Lower limit of the time window of BSS _m [Δt].
$\bar{\tau}^m$	Upper limit of the time window of BSS _m [Δt].
$\underline{\tau}^{\text{CCS}}$	Lower limit of the time window of CCS [Δt].
$\bar{\tau}^{\text{CCS}}$	Upper limit of the time window of CCS [Δt].
Q_k^{max}	Upper limit for total carrying capacity of BT _k [MWh].
M	A sufficiently large positive constant.
η^{ch}	Charging efficiency of batteries in W-CCS [%].
η^{dis}	Discharging efficiency of batteries in W-CCS [%].
$\rho_m^{\text{BSS}^*}$	Limit ratio for the abandonable demand of BSS _m [%].
e_m^{BSS}	Fully-charged battery demand of BSS _m [MWh].
p_t^{wind}	Wind power generation of W-CCS at time t [MW].
p_t^{plan}	Planned generation of W-CCS during time t [MW].
$\varepsilon^{\text{plan}^*}$	Limit for uncompleted generation plan at time t [%].
$\varepsilon^{\text{total}^*}$	Limit for total uncompleted generation plan [%].
$\rho^{\Delta E}$	Limits for fluctuations in FCB level in W-CCS [%].
\underline{E}/\bar{E}	Limits for the stored FCB level in W-CCS [MWh].

Manuscript received June 1, 2020; revised August 22, 2020; accepted September 24, 2020. Date of online publication November 20, 2020; date of current version December 30, 2020. This work was supported by the Fundamental Research Funds for the Central Universities (2572020BF04).

M. Ban (corresponding author, e-mail: mban2@iit.edu; ORCID: <https://orcid.org/0000-0003-0702-8295>) is with the College of Mechanical and Electrical Engineering, Northeast Forestry University, Harbin 150040, China.

J. Yu is with the Department of Electrical Engineering, Harbin Institute of Technology, Harbin 150001, China.

Y. Yao is with the National Renewable Energy Laboratory, Golden 80401, USA.

DOI: 10.17775/CSEEJPES.2020.02380

C. Variables

$p_t^{\text{plan}^*}$	Unfinished generation plan of W-CCS at time t [MW].
$p_t^{\text{grid}^*}$	Power bought from the grid at time t [MW].
$p_t^{\text{wind}^*}$	Wind curtailment of W-CCS at time t [MW].
$e_m^{\text{BSS}^*}$	Amount of unfinished FCB demand of BSS $_m$ [MWh].
$I_k^{m,n}$	Binary state variable of BT $_k$ between vertices m and n .
$I_k^{0,m}$	Binary state variable of BT $_k$ between W-CCS and n .
$I_k^{m, \mathcal{B} +1}$	Binary state variable of BT $_k$ between m and W-CCS.
e_k^m/e_k^n	FCB level of BT $_k$ when it leaves vertex m/n [MWh].
Δe_k^m	Battery exchange between BT $_k$ and BSS $_m$ [MWh].
$\Delta e_k^{r_{k,t}}$	Battery exchange between BT $_k$ and W-CCS ^R [MWh].
$I_{k,t}^{\text{stat}}$	Binary state variable for BT $_k$ starts delivery at time t .
$I_{k,t}^{\text{end}}$	Binary state variable for BT $_k$ ends delivery at time t .
τ_k^0	Period that BT $_k$ departs from W-CCS [Δt].
$\tau_k^{ \mathcal{B} +1}$	Period that BT $_k$ returns to W-CCS [Δt].
$e_{k,t}^{\text{start}}$	FCBs that BT $_k$ takes from W-CCS at time t [MWh].
$e_{k,t}^{\text{end}}$	FCBs that BT $_k$ gives to W-CCS at time t [MWh].
$\Delta e_k^{r_{k,t}}$	FCBs that BT $_k$ gets from W-CCS ^R at time t [MWh].
E_t	FCB level in the W-CCS at time t [MWh].
ΔE_t	Changes in the FCB level in W-CCS at time t [MWh].
I_t^{ch}	Binary state variable for battery charging at time t .
I_t^{dis}	Binary state variable for battery discharging at time t .
$I_k^{m,n}$	Binary travel state of BT $_k$ between vertices m and n .
p_t^{ch}	Charging power in W-CCS at time t [MW].
p_t^{dis}	Discharging power in W-CCS at time t [MW].
τ_d^m/τ_d^n	The period that BT $_k$ arrives at BSS $_m$ (BSS $_n$) [Δt].

D. Abbreviations and Symbols

dis/ch	Indicator for discharging/charging related parameters.
CCS	Centralized charging station.
BSCS	Battery swapping-charging system.
FCB	Fully-charged battery.
$(^*)/(\underline{^*})$	Upper and lower limits for item (*).

I. INTRODUCTION

TRANSPORTATION electrification will help to address various social and environmental problems associated with mass motorization and rapid urbanization, e.g., it benefits oil conservation, climate change mitigation, air quality improvement, and transit mode upgrading. Electric vehicles (EVs) play an essential role in realizing transportation electrification. During the last decade, EVs were rapidly developing, with the strong support of ambitious governments. By the end of 2017, the global stock of EVs surpassed 3 million [1], and their applications in power systems [2], [3], including energy storage [4], load shifting [5], frequency regulation [6], [7], operation reserves [8], [9], renewable energy integrating [10], [11], vehicle to grid [12], [13], transmission congestion relief [13], [14], resilience enhancing [15], and demand response [16], [17], etc., are widely studied. Yet environmental and charging concerns are still haunting the promotion of EVs.

On the one hand, with the rapid increase in charging demand of EVs, environmental concerns are gaining in importance in regions where power generation is primarily supplied by coal-fired power plants [17]. For example, China is the largest EV market in the world, while coal-fired power plants generated more than 70% of China's supplied electricity in 2018. In this setting, electricity supply EVs would produce large quantities of greenhouse gas and air pollutants. Even worse, some controlled EV charging solutions may reduce the generation cost, but they may also increase emissions primarily due to increased use of cheap coal-fired power plants [18], [19]. Therefore, EVs can represent clean electric mobility only if the potentially significant environmental concerns at the supply side can be effectively addressed via promoting renewable generation [20]. In this setting, charging EVs directly with renewables is undoubtedly the most effective approach.

On the other hand, rapidly growing charging demands of EVs require mass charging facilities [21]–[23]. However, it would be difficult to perform the widespread deployment of charging stations and charging piles in some highly populated regions, which have insufficient parking spaces and weak distribution grids [11], [12]. Network congestion, power losses, and large voltage drops limit deploying EV chargers in some old residential areas. Battery swapping technology can easily address these concerns [24], [25], and it is a promising alternative for promoting electric mobility [26], [27]. Thus, some populated countries with congested urban areas, such as India, Japan, and China, are early adopters that are pushing hard for battery swapping technology [28], [29], e.g., the State Grid Corporation of China is vigorously promoting the battery swapping station (BSS) option with pilot installations in multiple cities [30]–[33]. And very recently, a novel battery swapping-charging system (BSCS) was proposed. In this novel framework, modular EV batteries are centrally charged in a centralized charging station (CCS) and then dispatched to multiple BSSs via battery transporters (BTs) [34]–[36]. The CCS can be built nearby a substation and thus it will have little impact on local distribution grids [37]. Compared to the traditional charging stations [38] and BSSs [39], [40], the BSCS offers a more controllable and viable option for

transporting large quantities of electricity through the coupled transportation and power networks [41].

Based on the points mentioned above, a novel BSCS framework based on wind farms (hereinafter referred to as W-BSCS) is attracting attention. In a W-BSCS, the CCS can not only charge EV batteries with wind power but also support wind farms to supply high-quality electricity to the power grid. Reference [42] analyzes the benefits of the integration of wind farms and electric vehicle supporting facilities, and it points out that the integrated system will boom due to the development in dispersed wind power. In practice, dispersed wind power is expected to reach 20GW by 2020 in China, and most of the dispersed wind power projects will be built around urban areas. This will make the W-BSCS one of the most promising applications for promoting both wind power and EVs.

This paper focuses on the W-BSCS and establishes a joint optimal scheduling model, which optimally manages the W-BSCS to minimize the operational cost while satisfying the generation plan of the wind farm and the FCB demands of individual BSSs. It contributes to the literature by developing a joint optimization framework of battery charging/discharging scheduling of the CCS, and battery swapping scheduling between individual units, and the vehicle routing problem (VRP) of the BTs. Since the proposed scheduling model is an NP-hard problem, a heuristic solution method is designed. The major contributions of this paper are summarized as follows:

1) A W-BSCS consisting of a CCS, wind farms, BTs and BSSs is introduced. And several progressing technologies for simplifying the optimal scheduling of the W-BSCS is designed. Then, it formulates a comprehensive joint optimization model that simultaneously schedules battery charging/discharging, battery swapping, and VRP for the W-BSCS.

2) A heuristic method based on the exhaustive search and Genetic Algorithm is designed to solve the proposed NP-hard problem. Numerical results demonstrate the proposed model, and they indicate that the W-BSCS will benefit in promoting EVs and wind power. Also, it briefly discusses the potential expansion of the model for dealing with wind power uncertainty.

The rest of this paper is organized as follows. Section II introduces the framework of a W-BSCS system, and it also shows some processing technologies and assumptions for simplifying modeling. Section III formulates the joint optimal scheduling model, and Section IV provides a solution method. Section V performs numerical case studies with discussions, and the conclusion is provided in Section VI.

II. FRAMEWORK OF A W-BSCS SYSTEM

This section presents the framework of a W-BSCS, and then it develops several preprocessing assumptions and technologies for simplifying sequent joint optimal modeling.

A. Framework of a W-BSCS System

A W-BSCS framework is shown in Fig. 1. A CCS and wind farm form a W-CCS, where EV batteries can balance wind power fluctuations. The CCS primarily uses wind power

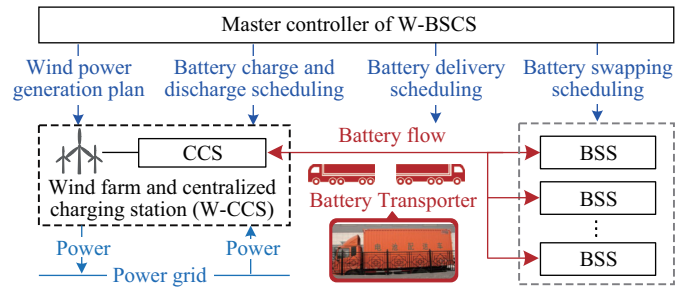


Fig. 1. Diagram of a W-BSCS.

to charge EV batteries, and it can also purchase electricity from the power grid when the wind power is insufficient. The massive FCBs of the W-CCS will be distributed to multiple BSSs to serve local EVs, by heavy trucks (referred to as battery transporter, BTs). The proposed W-BSCS represents a novel framework for performing energy & storage sharing and trading [43], [44], and it will help to address the environmental concerns on promoting EVs. Interested readers are referred to our previous study [37] for more details about the BSS and BSCS applications.

In the W-BSCS, the master controller is responsible for system-level management, and it establishes communication with individual BSSs, BTs and the W-CCS. In daily operations, the master controller collects various data (e.g., battery demand, wind power forecast, etc.) from individual units, and then it deals with them by solving a mathematical programming problem to find a day-ahead optimal scheduling solution. In other words, the master controller comprehensively controls the wind power generation plan and battery charging/discharging scheduling of the W-CCS, battery delivery scheduling of the BTs, and battery swapping scheduling among individual units.

The day-ahead scheduling of the W-BSCS primarily consists of two coupled parts. The first one is the battery charging and discharging, and it controls the CCS batteries to coordinate with the wind farm to complete the released generation plan. The second one is the VRP of the BTs, and it manages the delivery routes and battery swapping scheduling among the W-CCS and the BSSs (see Fig. 2). Note that the system-level scheduling will not cover detailed station-level management of the BSSs and demand patterns of EVs, and it assumes that the BSSs will address such issues before submitting their FCB demands.

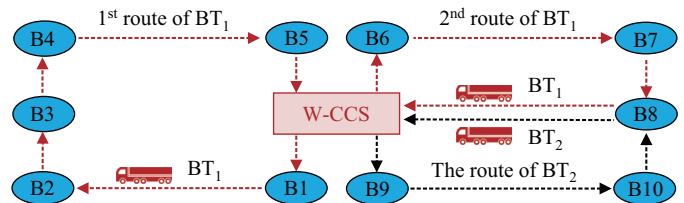


Fig. 2. An example with a W-CCS, 10 BSSs (B1–B10), and 2 BTs (BT₁–BT₂).

B. Preprocessing Assumptions and Technologies

To simplifying joint modeling of a W-BSCS, the employed preprocessing assumptions and technologies are as follows:

1) The battery swapping is only applied between two types of batteries, namely fully-charged batteries (FCBs) and empty ones, to improve energy exchange efficiency. And it assumes that individual units will prepare enough idle fully-charged and/or empty batteries for performing the following swapping operation, which is based on the assumption that the W-CCS and the BSSs can perform monotonic charging/discharging strategies for their local batteries connected in parallel [43].

2) The amount of energy exchange via battery swapping are presumed to be continuous variables. This is not the case in practical applications. However, if they are modeled as integer variables, they will badly aggravate the computation complexity. Similarly, the FCB level is presumed to be a continuous variable, and the stored energy of the W-CCS is represented by its FCB level, while battery charging and discharging operations will directly change the FCB level.

3) In order to facilitate the joint modeling of VRP of BTs and scheduling of W-CCS, the planning interval is discretized. Thereby, the time window of each BSS can be approximately represented by several consecutive time periods (see Fig. 3). For example, the 1st time window of B1 can be approximated as $[4\Delta t, 7\Delta t]$. Although this preprocessing will sacrifice some modeling accuracy, it can effectively reduce the complexity of the proposed problem.

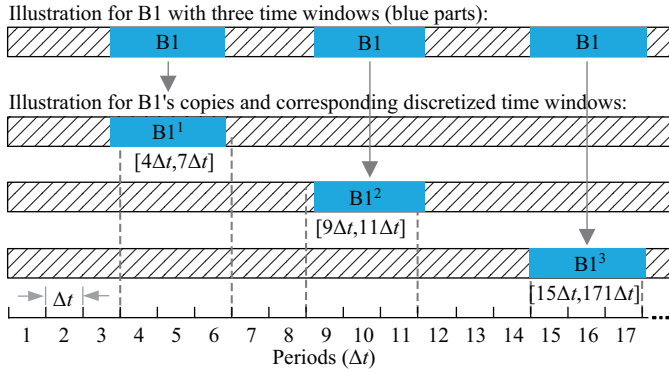


Fig. 3. Illustration for the copies and discretized time windows of a BSS (B1).

4) If a BSS has multiple battery requirements and corresponding multiple time windows, copies can be set for it. For example, if a BSS, e.g., B1, has three time windows, then three copies of it can be set, i.e., B1¹, B1², and B1³, which have the same sites as B1, but their time windows are the same as the 1st, 2nd and 3rd time windows of B1, respectively. Therefore, three BSSs with single time windows can replace B1, and the original VRP with multiple time windows is converted into VRP with a single time window that is easier to model and solve.

5) Copies are also set for the W-CCS, which are defined as supplementary stations (W-CCS^R). Each W-CCS^R has the same site of the W-CCS but only one-period time window that allows a BT to obtain a FCB supplement. W-CCS^R allows a BT to leave it to continue their subsequent delivery tasks. It is

distinguished from the W-CCS, which is the start and end of each BT's route. In this way, the original problem is simplified to an easier single depot VRP.

C. Joint Scheduling Description for a W-BSCS System

The joint optimal scheduling for a W-BSCS system can be described as: a fleet of BTs visit a set of customers (i.e., all BSSs and their copies) during their specific time windows, and each BT starts and ends its daily tour from the same one depot (i.e., W-CCS), which optimally charge and discharge the local batteries. The objective is to pick a cost-minimizing scheduling scheme to meet the generation plan of the wind farm and the FCB demand of the BSSs. This paper restricts its attention to the W-BSCS with one W-CCS, and the studied problem is a strict one-depot VRP. Moreover, the modeling of multiple W-CCSs is also an important subject, but it is beyond the scope of this paper, and we intend to consider it in a future study.

For notational convenience, the variables and parameters are described as: $\mathcal{B} = \{1, \dots, m(n), \dots\}$ denotes the set of BSSs and their copies, $\mathcal{K} = \{1, \dots, k, \dots\}$ denotes the set of BTs, $\mathcal{R}_k = \{r_{k,1}, \dots, r_{k,t}, \dots\}$ denotes the set of W-CCS^R, and vertices 0 and $|\mathcal{B}| + 1$ denote the W-CCS (i.e., the depot), in which every route starts at 0 and ends at $|\mathcal{B}| + 1$. To indicate that a vehicle routing set contains the respective instance of the depot, the set is subscripted with 0 or $|\mathcal{B}| + 1$, and thereby, $\mathcal{V}_0 = \mathcal{B} \cup \{0\}$ and $\mathcal{V}_{|\mathcal{B}|+1} = \mathcal{B} \cup \{|\mathcal{B}| + 1\}$. Then we can define the problem on a complete directed graph $(\mathcal{V}_{0,|\mathcal{B}|+1}, \mathcal{A})$ with the set of arcs $\mathcal{A} = \{(m, n) | m, n \in \mathcal{V}_{0,|\mathcal{B}|+1}, m \neq n\}$, in which each arc is associated with a specific travel cost and time. The binary state variable $I_k^{m,n}$ is equal to 1 if BT_k travels from vertex m to n , and 0 otherwise. The W-CCS can control at most $|\mathcal{K}|$ BTs to serve the BSSs, and each BSS at vertices $m \in \mathcal{B}$ has a FCB demand and corresponding time window $(\bar{\tau}^m, \underline{\tau}^m)$.

III. JOINT SCHEDULING MODEL FOR A W-BSCS SYSTEM

This section presents the MILP formulation of the proposed optimization model of the joint scheduling for the W-BSCS.

A. Objective

$$\min C_{\text{total}} = C_{\text{plan}} + C_{\text{BSS}} + C_{\text{delivery}} + C_{\text{grid}} + C_{\text{wind}} \quad (1)$$

where,

$$C_{\text{plan}} = \sum_{t \in \mathcal{T}} \gamma_t^{\text{plan}^*} p_t^{\text{plan}^*} \Delta t \quad (2)$$

$$C_{\text{BSS}} = \sum_{m \in \mathcal{B}} \gamma_m^{\text{BSS}^*} e_m^{\text{BSS}^*} \quad (3)$$

$$C_{\text{delivery}} = \sum_{k \in \mathcal{K}} \sum_{m \in \mathcal{V}_0, n \in \mathcal{V}_{|\mathcal{B}|+1}, m \neq n} \gamma_k^{m,n} I_k^{m,n} \quad (4)$$

$$C_{\text{grid}} = \sum_{t \in \mathcal{T}} \gamma_t^{\text{grid}^*} p_t^{\text{grid}^*} \Delta t \quad (5)$$

$$C_{\text{wind}} = \sum_{t \in \mathcal{T}} \gamma_t^{\text{wind}^*} p_t^{\text{wind}^*} \Delta t \quad (6)$$

The objective minimizes the sum of the penalty for failure in completing the power generation plan, the penalty for failure

in meeting the battery swapping demand, the delivery cost of the BTs, the cost for buy power from the power grid, and the virtual penalty for wind curtailment. Note that the battery transportation cost is not modeled in detail but covered by the delivery cost of BTs.

B. Constraints for Delivery Routes

The constraints for delivery routes are similar to traditional VRP problems, (7) and (8) state that each BSS is visited at least once and at most N_{\max} times by BTs, (9) states the flow conservation (a BT that enters a BSS site must leave), (10) denotes that each BT must return to CS, (11) states that each BT can be assigned at most one trip, and (12) limits the maximum delivery distance for each BT. In addition, the unreasonable delivery routes can be relaxed by assigned extreme values.

$$\sum_{k \in \mathcal{K}} \sum_{n \in \mathcal{B}} I_k^{m,n} \geq 1 \quad \forall m \in \mathcal{V}_0, m \neq n \quad (7)$$

$$\sum_{k \in \mathcal{K}} \sum_{n \in \mathcal{B}} I_k^{m,n} \leq N_{\max} \quad \forall m \in \mathcal{V}_0, m \neq n \quad (8)$$

$$\sum_{k \in \mathcal{K}} \left(\sum_{m \in \mathcal{V}_0, m \neq n} I_k^{m,n} - \sum_{m \in \mathcal{V}_{|\mathcal{B}|+1}, m \neq n} I_k^{n,m} \right) = 0 \quad \forall n \in \mathcal{V} \quad (9)$$

$$\sum_{n \in \mathcal{B}} I_k^{0,n} - \sum_{m \in \mathcal{B}} I_k^{m,|\mathcal{B}|+1} = 0 \quad \forall k, m \neq n \quad (10)$$

$$\sum_{n \in \mathcal{B}} I_k^{0,n} \leq 1 \quad \forall k \quad (11)$$

$$\sum_{n \in \mathcal{V}_{|\mathcal{B}|+1}} I_k^{m,n} d^{m,n} \leq D_k^{\max} \quad \forall k, \quad \forall m \in \mathcal{V}_0, m \neq n \quad (12)$$

C. Constraints for Time Windows

Constraints (13) and (14) guarantee BT_k visits each BSS location within the specified time window, (15) tracks the time that BT_k arrives at each BSS, and (16) ensures that BT_k returns to the CS during its operational periods. The proposed approach assumes that the battery swapping operation can be completed within one period, that is, if a BT arrives at a BSS, it will complete the battery swapping operation and then leave within the same time period.

$$-M(1 - I_k^{m,n}) + \tau^n \leq \tau_k^n \quad \forall k, \quad \forall m \in \mathcal{V}_0, \quad \forall n \in \mathcal{V} \quad (13)$$

$$\tau_k^n \leq M(1 - I_k^{m,n}) + \bar{\tau}^n \quad \forall k, \quad \forall m \in \mathcal{V}_0, \quad \forall n \in \mathcal{V} \quad (14)$$

$$\tau_k^m + \Delta \tau_k^{m,n} I_k^{m,n} \leq \tau_k^n + M(1 - I_k^{m,n}) \quad \forall k, \quad \forall m \in \mathcal{V}_0, \quad \forall n \in \mathcal{V}_{|\mathcal{B}|+1} \quad (15)$$

$$\underline{\tau}^{\text{CCS}} \sum_{n \in \mathcal{B}} I_k^{0,n} \leq \tau_k^0 \leq \tau_k^{|\mathcal{B}|+1} \leq \bar{\tau}^{\text{CCS}} \sum_{n \in \mathcal{B}} I_k^{n,|\mathcal{B}|+1} \quad \forall k \quad (16)$$

D. Constraints for Battery Swapping Between BT and BSS

A BT unloads FCBs and loads empty ones at the BSSs: (17) and (18) tracks the remaining amounts of the FCBs when BT_k travels between BSSs m and n , while (19) limiting the amount of the FCBs that BT_k can supply to a BSS; (20) limits the total carrying capacity of BT_k ; (21) states the FCB demand of a BSS can be met by swapping batteries with all BTs and

parts of its demand can be abandoned, and (22) limits the total amount of abandoned FCB demand of BSS_m .

$$0 \leq e_k^n \leq e_k^m + M(1 - I_k^{m,n}) - \Delta e_k^m \quad \forall k, \quad \forall m \in \mathcal{V}_0, \quad \forall n \in \mathcal{V}_{0,|\mathcal{B}|+1} \quad (17)$$

$$e_k^m + M(I_k^{m,n} - 1) - \Delta e_k^m \leq e_k^n \quad \forall k, \quad \forall m \in \mathcal{V}_0, \quad \forall n \in \mathcal{V}_{|\mathcal{B}|+1} \quad (18)$$

$$0 \leq \Delta e_k^m \leq \Delta \bar{e}_k^m \sum_{n \in \mathcal{V}_0} I_k^{n,m} \quad \forall k, \quad \forall m \in \mathcal{B} \quad (19)$$

$$0 \leq e_k^m \leq Q_k^{\max} \quad \forall k, \quad \forall m \in \mathcal{V}_{0,|\mathcal{B}|+1} \quad (20)$$

$$e_m^{\text{BSS}} = e_m^{\text{BSS}^*} + \sum_{k \in \mathcal{K}} \Delta e_k^m \quad \forall m \in \mathcal{B} \quad (21)$$

$$0 \leq e_m^{\text{BSS}^*} \leq \rho_m^{\text{BSS}^*} e_m^{\text{BSS}} \quad \forall m \in \mathcal{B} \quad (22)$$

E. Constraints for Battery Swapping Between BT and W-CCS

As for the W-CCS, equations (23)–(25) link the relationships between the period that BT_k departs from (returns to) the W-CCS and its delivery task states. For example, if BT_k starts (ends) its delivery at period t , then $I_{k,t}^{\text{start}}$ (or $I_{k,t}^{\text{end}}$) will be 1, and then the period τ_k^0 or $\tau_k^{|\mathcal{B}|+1}$ that BT_k departs from (or returns to) the W-CCS is t ; (26) and (27) define the amount of FCBs that BT_k can load when it departs from the W-CCS, while (28) and (29) define the final amount of FCBs when BT_k returns to the W-CCS. Note that if BTs only take empty batteries from the BSSs and then gives them all to the W-CCS, then (28) and (29) can be omitted.

$$\sum_{t \in \mathcal{T}} I_{k,t}^{\text{start}} t = \tau_k^0 \quad \forall k \quad (23)$$

$$\sum_{t \in \mathcal{T}} I_{k,t}^{\text{end}} t = \tau_k^{|\mathcal{B}|+1} \quad \forall k \quad (24)$$

$$\sum_{t \in \mathcal{T}} I_{k,t}^{\text{start}} = \sum_{t \in \mathcal{T}} I_{k,t}^{\text{end}} = \sum_{n \in \mathcal{B}} I_k^{0,n} \quad \forall k \quad (25)$$

$$0 \leq e_{k,t}^{\text{start}} \leq I_{k,t}^{\text{start}} M \quad \forall k \quad (26)$$

$$\sum_{t \in \mathcal{T}} e_{k,t}^{\text{start}} = e_k^0 \quad \forall k \quad (27)$$

$$0 \leq e_{k,t}^{\text{end}} \leq I_{k,t}^{\text{end}} M \quad \forall k \quad (28)$$

$$\sum_{t \in \mathcal{T}} e_{k,t}^{\text{end}} = e_k^{|\mathcal{B}|+1} \quad \forall k \quad (29)$$

As for W-CCS^{R} s, the constraint (30) states that the BT_k can obtain FCB replenishment from a W-CCS^{R} , and (31) restricts the lower and upper limits for the FCB replenishment, and (32) limits the total carrying capacity of BT_k . Note that the battery swapping operation between BT_k and a W-CCS^{R} is the same as that between BT_k and a BSS, while the difference is that BT_k can load FCBs at a W-CCS^{R} and continue its sequent delivery task.

$$0 \leq e_k^m \leq e_k^{r_{k,t}} + M(1 - I_k^{r_{k,t},m}) + \Delta e_k^{r_{k,t}} \quad \forall k, \quad \forall m \in \mathcal{B}, \quad \forall r_{k,t} \in \mathcal{R}_k \quad (30)$$

$$0 \leq \Delta e_k^{r_{k,t}} \leq \Delta \bar{e}_k^{r_{k,t}} \sum_{m \in \mathcal{B}} I_k^{r_{k,t},m} \quad \forall k, \quad \forall r_{k,t} \in \mathcal{R}_k \quad (31)$$

$$0 \leq e_k^{r_{k,t}} \leq Q_k^{\max} \quad \forall k, \quad \forall m \in \mathcal{B}, \quad \forall r_{k,t} \in \mathcal{R}_k \quad (32)$$

Remark: $I_{k,t}^{\text{start}}$, $I_{k,t}^{\text{end}}$, $e_{k,t}^{\text{start}}$, $e_{k,t}^{\text{end}}$, $I_{k,t}^{r_{k,t},m}$ and $e_{k,t}^{r_{k,t}}$ are complicating variables linking independent W-CCS scheduling and VRP subproblems.

F. Constraints for CCS Operation

The equation (33) states the power balance in the CCS, and it shows that when the battery storage can hardly balance the wind power and the generation plan, wind curtailments or generation violations will occur. Note that the electricity bought from the power grid has no participation in the (33). Equations (34)–(36) limits the charging and discharging operations; (37) limits the wind curtailment and (38) limits the power that the W-CCS can buy from the grid, (39) and (40) limits the failed plan during period t and the total amount of the failed plan.

$$p_t^{\text{wind}} + p_t^{\text{dis}} - p_t^{\text{ch}} - p_t^{\text{plan}} = p_t^{\text{wind}^*} - p_t^{\text{plan}^*} \quad \forall t \quad (33)$$

$$\underline{p}_t^{\text{ch}} I_t^{\text{ch}} \leq p_t^{\text{ch}} \leq \bar{p}_t^{\text{ch}} I_t^{\text{ch}} \quad \forall t \quad (34)$$

$$\underline{p}_t^{\text{dis}} I_t^{\text{dis}} \leq p_t^{\text{dis}} \leq \bar{p}_t^{\text{dis}} I_t^{\text{dis}} \quad \forall t \quad (35)$$

$$I_t^{\text{ch}} + I_t^{\text{dis}} \leq 1 \quad \forall t \quad (36)$$

$$0 \leq p_t^{\text{wind}^*} \leq p_t^{\text{wind}} \quad \forall t \quad (37)$$

$$\underline{p}_t^{\text{grid}} \leq p_t^{\text{grid}} \leq \bar{p}_t^{\text{grid}} \quad \forall t \quad (38)$$

$$0 \leq p_t^{\text{plan}^*} \leq \varepsilon_t^{\text{plan}^*} p_t^{\text{plan}} \quad \forall t \quad (39)$$

$$\sum_{t \in T} p_t^{\text{plan}^*} \leq \varepsilon_{\text{total}}^{\text{plan}^*} \sum_{t \in T} p_t^{\text{plan}} \quad \forall t \quad (40)$$

Constraints (41) and (42) track the FCB level changes of the W-CCS when BT_k leaves and returns, where E_0 is its initial value, and (43) limits the lower and upper limits of the FCB level, while (44) avoiding the possible end-of-horizon effects of finite-horizon scheduling models by limiting the upper/lower fluctuations in the FCB level in the W-CCS.

$$E_t = E_0 + \sum_{v \in (1, \dots, t)} \left[\left(\eta^{\text{ch}} p_v^{\text{grid}} + \eta^{\text{ch}} p_v^{\text{ch}} - \frac{p_v^{\text{dis}}}{\eta^{\text{dis}}} \right) \Delta t - \Delta E_v \right] \quad \forall t \quad (41)$$

$$\Delta E_t = \sum_{k \in \mathcal{K}} (e_{k,t}^{\text{start}} - e_{k,t}^{\text{end}}) + \sum_{k \in \mathcal{K}} \Delta e_k^{r_{k,t}} \quad \forall t \quad (42)$$

$$\underline{E} \leq E_t \leq \bar{E} \quad \forall t \quad (43)$$

$$E_0 (1 - \rho^{\Delta E}) \leq E_{|\mathcal{T}|} \leq E_0 (1 + \rho^{\Delta E}) \quad (44)$$

IV. SOLUTION METHODOLOGY

The proposed problem is modeled in the MILP formulation, however, due to the VRP being a NP-hard problem, it can hardly be directly solved using commercial solvers. Thus, this paper employs the exhaustive search and the Genetic Algorithm to solve the proposed problem.

A. Exhaustive Search

Exhaustive search, also known as brute-force search, is a very general solving technique and algorithmic paradigm that consists of systematically enumerating all possible candidates for the solution and checking whether each candidate satisfies the statements of the targeted problem. Although the exhaustive search method is simple to implement and will always find an optimal solution, if it exists, its computing cost is

proportional to the number of candidate solutions, which tends to grow quickly as the size of the problem increases, i.e., combinatorial explosion. Therefore, the exhaustive search is typically used when the problem size is limited. In this paper, the exhaustive search is only responsible for searching the periods that BTs depart from the W-CCS (i.e., τ_k^0). That is exactly what the exhaustive search is good at, and thus it can be easily employed to solve the problem.

Specifically, the time range that a BT can depart from the W-CCS to start its delivery tasks is limited within the operational periods of the W-CCS, and thus the exhaustive search can easily search all possible departure periods (τ_k^0) of BT_k and form a set of feasible solutions. In addition, an effective way to speed up the exhaustive search is to reduce its search space, i.e., the set of candidate solutions, by using problem-specific heuristics. And thus, this paper first only considers part of the conditions of the problem to obtain an augmented set of possible departure period solutions. Next, each group of the possible departure period solutions matches the delivery routes, which are obtained by the Genetic Algorithm, and it judges if there is a set of feasible solution combinations. Then, the objective values of all feasible solution combinations will be compared to find the optimal one. The relationship between the exhaustive search and the Genetic Algorithm, as well as their stopping criteria, will be discussed in Section IV.C.

B. Genetic Algorithm

The Genetic Algorithm is a typical method used in solving VRPs. Its main steps include encoding, decoding, and calculating fitness [44]. It continuously forms new populations, via selection, crossover, mutation operations, in each iteration process, and finally, it will obtain an approximate optimal solution.

Here, we would like to introduce the coding and decoding processes of the employed Genetic Algorithm. Unlike the traditional VRPs, the proposed model involves issues, such as the number of FCBs that a BT takes from the W-CCS and the BSS set. This will dramatically increase the difficulty of the coding operation, and the traditional coding methods can hardly meet the new requirements. Therefore, the segmented chromosome hybrid coding method is used, and the chromosome is divided into two parts: the delivery route based on integer coding and the FCB amount based on floating-point coding. A simple illustration of the employed coding method is given in Fig. 4.

The other parts of the employed Genetic Algorithm are the same as its typical applications, and thus this paper has no specific introduction for them, while the interested readers are referred to reference [44] for more details. Besides, in order to reduce the size of the formulation, we also employ some preprocessing techniques to eliminate infeasible routes in the scheduling for the W-BSCS and apply a dominance rule to find non-dominated routes [46].

C. Relationship Between Exhaustive Search and Genetic Algorithm

Figure 5 illustrates the brief solution processes of the proposed problem, which primarily depends on cooperation between the exhaustive search and the Genetic Algorithm. On

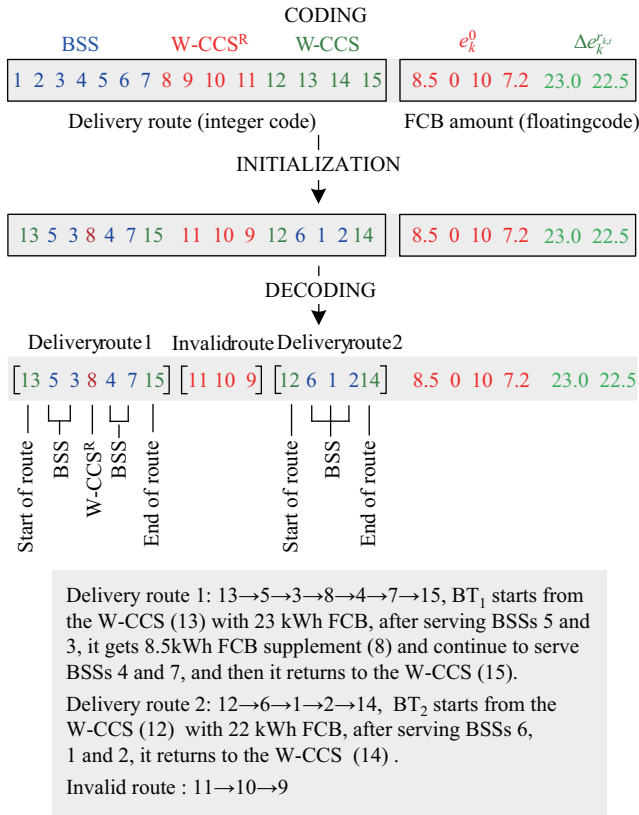


Fig. 4. Illustration of coding and decoding operation in the Genetic Algorithm.

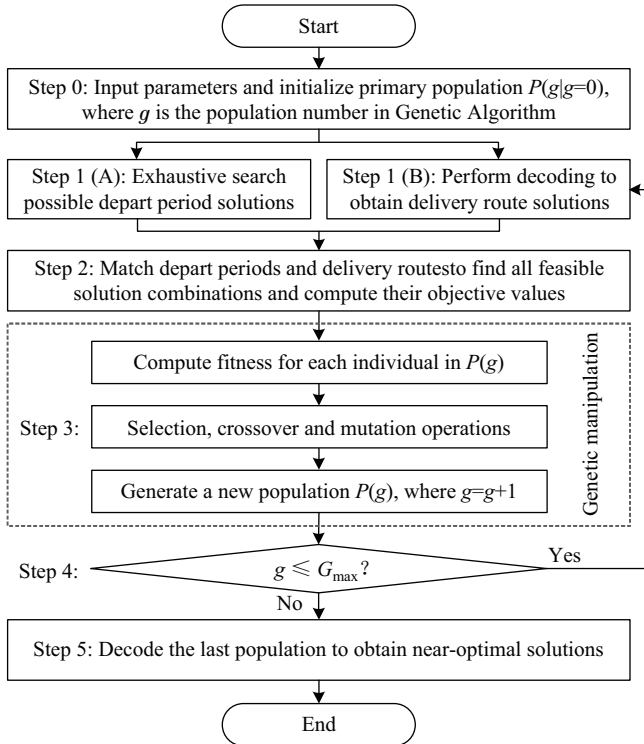


Fig. 5. Illustration of the solution process.

the one hand, the exhaustive search finds all possible depart period (τ_k^0) solution candidates for the BTs, see Step 1 (A).

On the other hand, the Genetic Algorithm finds other decision variables (e.g., $I_k^{m,n}$) and corresponding delivery routes of BTs, see Step 1 (B). During each iteration process of the Genetic Algorithm, the effective delivery routes, which are obtained by decoding the current population, will match all the ready-made depart periods (Step 2), and then all the feasible combinations are compared to find the optimal one, whose objective value will be used as the fitness of the current population in the Genetic Algorithm (Step 3). The stopping criteria of the Genetic Algorithm depends on the total number of generations (i.e., G_{max} , Step 4), while the exhaustive search stops as long as all the possible solution candidates are found in Step 1. Finally, it will obtain the approximate optimal solutions of the problem by decoding the last-generation population, see Step 5.

V. CASE STUDIES

This section presents numerical examples that demonstrate the effectiveness of the proposed approach, show the benefits of the W-BSCS (Section A), and gives some discussion about wind power uncertainty (Section B).

A system consisting of a W-CCS and 14 BSSs (see Fig. 6) is employed, and the delivery routes for the BTs are modified from the sets of a benchmark problem for VRP. The W-CCS controls 7 BTs to serve the BSSs. Each BC has a 3360 kWh maximum battery carrying capacity and can take about 50 standard batteries with a capacity of a 67.2 kWh package. And the maximum driving distance of each BT is 252 km, while the driving price is assumed as \$1.25/km. The total number of simulation periods is 96, and the length of each period (Δt) is 15 minutes. The W-CCS is based on a 66 MW wind farm, while the wind power generation plan (p_t^{plan}) and forecasted wind power (p_t^{wind}) of the W-CCS are shown in Fig. 7. The specific data for p_t^{plan} , p_t^{wind} , $d^{m,n}$, $\Delta\tau_k^{m,n}$, p_m^{BSS} and time windows are given in motor.ece.iit.edu/data/WBSCS. The studied W-BSCS can meet daily electricity requirements of 7600 private electric cars [14], and thus has the potential to serve city-level EV clusters using renewable energy.

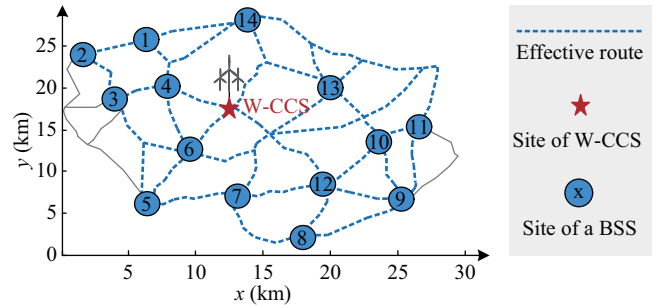


Fig. 6. Illustration for the W-BSCS used for the case study.

The penalty price (γ_t^{plan*}) for failing to complete the original power generation plan (P_t^{plan*}) is 1.5 times the price of the wind power generation plan (P_t^{plan}). The benchmark price of the wind power generation plan is set as \$100/MWh, while the prices during peak periods (40–60, 72–84) and valley periods (0–28, 92–96) are 1.5 and 0.5 times the benchmark price. The

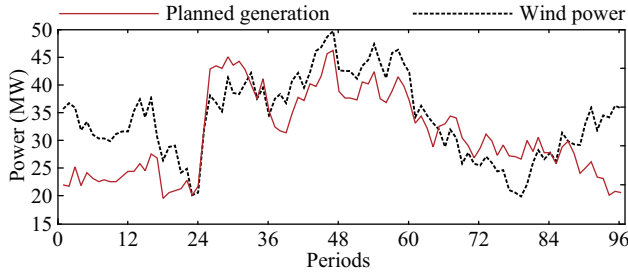


Fig. 7. Planned generation and forecasted wind power of the W-CCS during the whole horizon.

penalty price ($\gamma_t^{\text{BSS}^*}$) for failing to complete the FCB demand is twice the revenue (\$95/MWh) of providing battery swapping services to BSSs, i.e., \$190/MWh. In order to simplify the analysis, this study has no consideration of the arbitrage of using EV battery storage to participate in the time-of-use price mechanism, while the price that the W-CCS purchases electricity from the power grid ($\gamma_t^{\text{grid}^*}$) is set as \$240/MWh, and the wind curtailment price ($\gamma_t^{\text{wind}^*}$) is \$11.5/MWh.

The maximum battery capacity of the W-CCS is 50 MWh, and the corresponding maximum stored FCB level is 48.75 MWh. The maximum charging and discharging powers are 15 MW and 10 MW, and the charging/discharging loss is 2.5%, while the other key parameters are listed in Table I. In addition, the parameters of the Genetic Algorithm are listed in Table II, which are selected based on multiple simulation experiments with different values.

TABLE I
DATA FOR THE CASE STUDY

Item	Value	Item	Value	Item	Value
N_{\max}	3	$\varepsilon^{\text{plan}^*}$	10%	\bar{E}	48.75 MWh
$\Delta \bar{e}^m$	1.25 MWh	$\varepsilon_{\text{total}}^{\text{plan}^*}$	5%	$\rho \Delta E$	15%
\bar{p}^{grid}	5 MW	E_0	25 MWh	η^{ch}	97.5%
$\rho_{\text{m}}^{\text{BSS}^*}$	5%	\underline{E}	2 MWh	η^{dis}	97.5%

TABLE II
PARAMETERS OF THE GENETIC ALGORITHM

Item	Description	Value
N	Population size of chromosomes	200
G_{\max}	Maximum number of generations	300
N_e	Population size of elite chromosomes	20
P_c	Probability of crossover	0.9
P_v	Probability of mutation	0.1

A. Results with Forecasted Wind Power

Considering the randomness in the mutation and crossover operations of the Genetic Algorithm, the proposed problem is repeatedly solved six times, and the solution time of the individual tests varies from 15 to 22 minutes. The iteration processes of all the tests are compared in Fig. 8, which shows that the Genetic Algorithm begins to converge after 200-250 iterations, and when the iteration exceeds 275 times, the resulted objective value no longer significantly changes. Fig. 8 shows that the objective value of each test trends to converge to a certain value, and the difference between the results of individual tests is within a gap no larger than 5%.

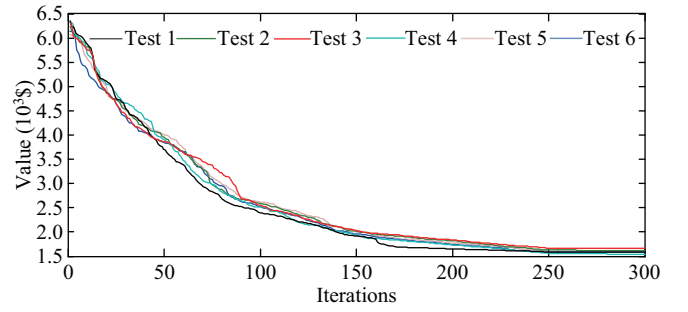


Fig. 8. Illustration for the interactive processes in individual tests.

And thus, it demonstrates the effectiveness of the employed Genetic Algorithm.

Table III compares the detailed results of the individual tests in Fig. 8, respectively. Since the W-CCS can effectively balance the difference between the power generation plan and the wind power, all the dispatch schemes in Table III have completed most of the power generation plan and thus avoid high penalty costs. In addition, the FCB demands of all the BSSs are also basically met. Test 4 performs better than all the other tests, since it completes all the expected generation plans and has the lowest wind curtailment, and it is used in the following analysis.

TABLE III
THE OBJECTIVE VALUES IN INDIVIDUAL SIMULATIONS

Test No.	C_{plan} (\$)	C_{BSS} (\$)	C_{delivery} (\$)	C_{wind} (\$)	C_{total} (\$)
1	0	28.6	1493.4	56.1	1578.1
2	86.5	56.4	1412.2	68.5	1623.6
3	104.5	0	1502.8	77.7	1685.0
4	0	15.2	1473.8	55.6	1544.6
5	180.0	38.2	1334.9	65.1	1618.2
6	0	34.3	1498.3	56.7	1589.3

In the case study, if the wind farm has no cooperation with a CCS, the wind curtailment will be 100.4 MWh, which accounts for 12.2% of the total wind power generation. In comparison, wind curtailment can be significantly reduced to 5.1 MWh after equipping a CCS. The FCB demand of BSSs (72.0 MWh) can be fully satisfied by wind power. Using recycled wind power, the proposed W-CCS can serve about 7600 EVs using wind power. In this way, it will help to enhance the cleanliness of electricity consumed by EV clusters. At the same time, the W-CCS will improve its income. For example, if the CCS charges the BSSs at a price of \$95/MWh, then it can get at most \$6840 for providing battery swapping service to the BSSs. In contrast, if the wind farm has no cooperation with a CCS, then it will hardly complete the 27.2 MWh generation plan, and therefore, it has to pay \$3067.3, which accounts for 3.9% of its total generation income. This will badly influence the economic performance of the wind farm.

Figure 9 shows the charging/discharging power, the stored FCB level, and the exported FCBs of the W-CCS. During high wind power periods, such as periods 0–12, the W-CCS will continuously charge the batteries. Otherwise, during the periods that the wind power is insufficient, the W-CCS will discharge the batteries to support the wind farm to complete the generation plan. In addition, since the W-CCS can output

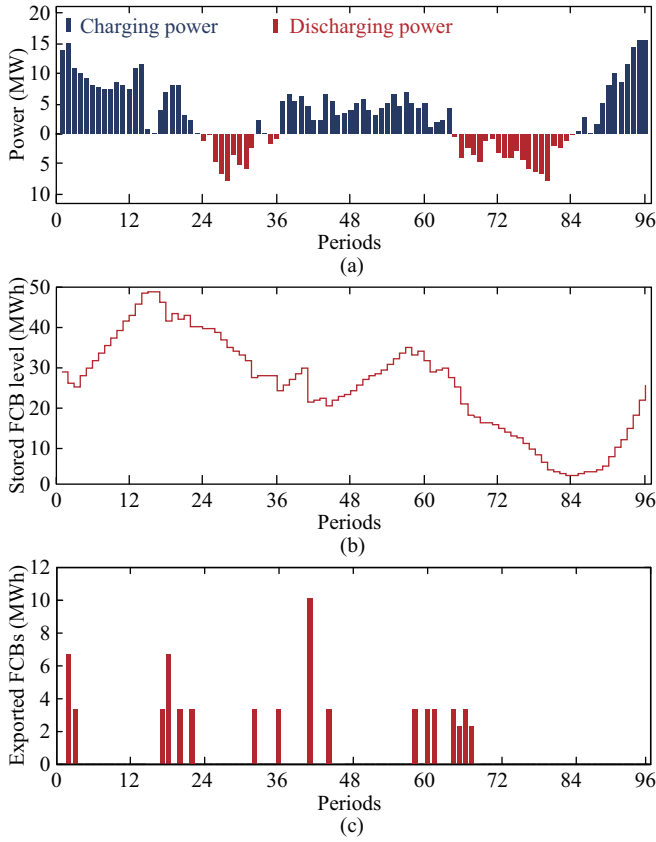


Fig. 9. Simulation results for power components, the stored FCB level and the exported FCBs in the W-CCSs.

its FCBs to the BSSs and then receive empty EV batteries in return, it can always keep enough storage capacity to absorb the high wind power during low load periods. In this way, the W-CCS and the BSSs at different sites can perform effective energy and storage sharing, and thereby, the proposed W-BSCS can achieve multiple benefits.

The delivery routes of BTs are shown in Table IV, in which W represents the W-CCS and B represents a BSS. Table IV demonstrates how the W-CCS uses the transportation system to enhance its operational flexibility. For example, during the 2nd period, BT₁ and BT₂ begin their delivery task. Therefore, after serving the BSSs, i.e., B4, B14, B13 . . . , they can return to the W-CCS very early, in addition to taking away FCBs, they will timely take back empty EV batteries to the W-CCS, who will correspondingly supply more storage capacity for aborting additional wind power.

B. Results with Volatile Wind Power

To take wind power uncertainty into account, the wind power is assumed to follow a normal distribution $N(\mu, \sigma)$ with expected value μ equal to the forecasted wind power at each period and standard deviation (volatility) σ , which is a percentage of μ , i.e., 2% in this case. Then the LHS and scenario reduction techniques generate 10 scenarios according to $N(\mu, \sigma)$ [46]. In each scenario, a wind power generation profile is considered using the solutions of all the tests, and then the average costs are given in Table V. To keep consistent

TABLE IV
VRP RESULTS FOR THE BTs

BT	Routing of BTs	τ_k^0
BT ₁	W-B4-B14-B13-B6-W-B12-B7-B5-B6-B4-W-B13-B10-B9-B12-W	2
BT ₂	W-B4-B1-B2-B3-B6-W-B13-B10-B9-B12-B7-W-B12-B9-B8-B7-B6-W	2
BT ₃	W-B14-B5-B7-B8-B12-W-B14-B1-B2-B3-B4-W-B4-B3-B5-B7-B12-W	3
BT ₄	W-B12-B8-B9-B10-B13-W-B12-B9-B11-B10-B13-W-B14-B1-B2-B3-B5-B6-W	17
BT ₅	W-B12-B9-B10-B13-B14-W-B6-B5-B7-B8-B12-W-B7-B8-B9-B11-B10-W	18
BT ₆	W-B13-B10-B9-B8-B12-W-B14-B13-B10-B12-B7-W-B12-B9-B10-B13-B14-W	20
BT ₇	W-B14-B13-B7-B5-B6-W-B4-B1-B2-B3-B6-W-B7-B8-B9-B10-B13-W	22

TABLE V
AVERAGE OBJECTIVE VALUES IN 10 SCENARIOS WITH EACH SIMULATION

Test No.	C_{plan}^i (\$)	C_{BSS}^i (\$)	C_{delivery}^i (\$)	C_{wind}^i (\$)	C_{total}^i (\$)
1	112.1	59.2	1493.4	96.2	1760.9
2	122.5	76.6	1412.2	88.5	1699.8
3	109.3	65.2	1502.8	97.7	1775.0
4	127.8	65.2	1473.8	95.5	1762.3
5	186.2	56.4	1334.9	105.0	1682.5
6	102.3	65.2	1498.3	95.5	1761.3

with the above deterministic analysis, the following study has no consideration that the W-CCS purchases electricity from the power grid.

An interesting finding is that the scheduling scheme in Test 4 may no longer necessarily perform better than other schemes in the stochastic scenarios (see Table V). This outcome indicates that modifying the scheduling schemes to consider wind power uncertainty is essential for achieving more practical benefits of the proposed W-CCS. In a future study, the proposed model will be expanded into stochastic models for addressing issues, such as uncertainties and fluctuations in wind power.

The proposed approach can be expanded to consider wind power uncertainty by referring to typical two-stage stochastic optimization methods. Generally, in a two-stage stochastic optimization model, decisions are divided into two categories: here-and-now versus wait-and-see decisions [47]. Using similar ideas, a posterior approach is employed to solve our problem. For the sake of conciseness, the problem is shown as:

$$\min_{\mathbf{x} \in \Omega_1, \mathbf{y} \in \Omega_2, \zeta \in \Omega_3} \{ \mathbf{c}^T \mathbf{x} + E_{\zeta} [Q(\mathbf{x}, \mathbf{y}, \zeta)] \mid \mathbf{A}\mathbf{x} + \mathbf{B}\mathbf{y} + \mathbf{H}\zeta \leq \mathbf{d} \} \quad (45)$$

where \mathbf{x} , \mathbf{y} and ζ represent the VRP related integer variables (i.e., routing selections of BTs), the other variables (i.e., charge and discharge states, charge and discharge power, changes in FCB levels, etc.), and uncertain vector (i.e., wind power), while Ω_1 , Ω_2 and Ω_3 represent the corresponding sets of feasible decisions, respectively; $(\mathbf{c}, \mathbf{A}, \mathbf{B}, \mathbf{H}, \mathbf{d})$ represent parameters for modeling the problem; and the second term in the objective is the expected cost considering uncertainty. The employed approach is as follows:

1) Obtaining Integer Variables

With the forecasted wind power (ζ^0), the heuristic method in Section IV will find a group of solutions by solving the following deterministic problem

$$\min_{\mathbf{x} \in \Omega_1, \mathbf{y} \in \Omega_2} \{ \mathbf{c}^T \mathbf{x} + Q(\mathbf{x}, \mathbf{y}, \zeta) \mid A\mathbf{x} + B\mathbf{y} + H\zeta \leq \mathbf{d}, \zeta = \zeta^0 \} \quad (46)$$

and then the obtained solution of the VRP related integer variables \mathbf{x} , which is denoted as \mathbf{x}^* , are saved. Accordingly, after solving the problem multiple times, it will form a possible solution set (Ω_1^*) of \mathbf{x}^* .

2) Checking Feasibility

Since most integer variables (\mathbf{x}) have been set to fixed values (\mathbf{x}^*), the size of the remaining part of the problem is greatly reduced, and then it can be directly solved by general MILP solvers. For computational purposes, discrete simulated scenarios are employed to represent the uncertainty of ζ that follows a known probability distribution, e.g., $N(\mu, \sigma)$, and in this setting, for each realization scenario (i.e., s) of the uncertain ζ , a new formulation is as

$$\min_{\mathbf{x} \in \Omega_1^*, \mathbf{y} \in \Omega_2, \zeta \in \Omega_3} \{ Q(\mathbf{x}, \mathbf{y}, \zeta^s) \mid A\mathbf{x}^* + B\mathbf{y} + H\zeta^s \leq \mathbf{d}, \mathbf{x} = \mathbf{x}^* \} \quad (47)$$

where ζ^s presents wind power in scenario s . If it (47) has no solutions, then \mathbf{x}^* is not a feasible solution in scenario s , and consequently, it will be removed from Ω_1^* . Furthermore, other options, such as checking the available probability of the solution and then determine whether it is a chance-constrained feasible one, can also be employed according to practical requirements.

3) Comparing Solutions

Using the same realization set of ζ , individual feasible solution \mathbf{x}^* in the remaining Ω_1^* will be compared. And a scenario-based stochastic model with non-anticipative constraints is as

$$\min_{\mathbf{x} \in \Omega_1^*, \mathbf{y} \in \Omega_2, \zeta \in \Omega_3} \left\{ \sum_{s \in S} \text{Pr ob}^s Q(\mathbf{x}, \mathbf{y}, \zeta^s) \mid A\mathbf{x}^* + B\mathbf{y} + H\zeta^s \leq \mathbf{d}, \mathbf{x} = \mathbf{x}^* \right\} \quad (48)$$

where Pr ob^s is the probability of scenarios s . After testing individual group of \mathbf{x}^* with all the scenarios, the solution which has the best performance can be selected as the final one.

Note that the proposed posterior approach has its inherent flaws, in the sense of optimization, since it can hardly ensure the optimality of the selected solution. Still, it can make our model more practical when considering wind power uncertainty. Using the above approach and forecasted wind power, 30 groups of possible solutions are obtained, and they are tested by wind power scenario sets with different standard deviation (volatility) values, which are generated according to $N(\mu, \sigma)$. Fig. 10 illustrates the feasibility checking results under different standard deviation values equal to 1, 2, ..., and 10 percent, respectively (see 100% case). In addition, Fig. 10 also shows the counterpart results in which a case a possible

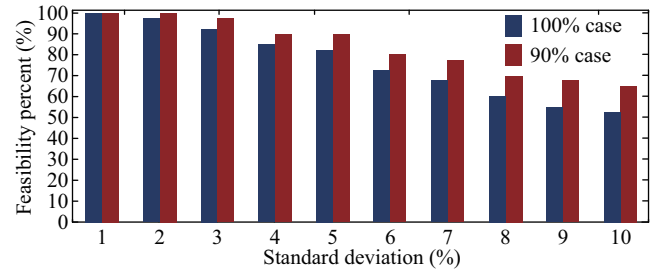


Fig. 10. Feasibility checking results of solutions under different levels of wind power uncertainty represented by increased standard deviation values.

solution is defined as a feasible one as long as it can meet the requirements of 90% of the scenarios (see 90% case). The results illustrate that the proposed approach helps to eliminate unusable solutions while meeting different levels of robust requirements, and thus, it will improve the reliability of the proposed approach.

To further verify the benefits of the proposed approach, the best one of the above 30 solutions is selected, using the scenario set with σ equals to 5%. Then it is compared with the 6 solutions in Section A, and Fig. 11 shows the comparing results. The new solution performs better than the others, e.g., its cost results distribute in a more concentrated interval and it also has the lowest median value. The results demonstrate that the proposed approach, even though it has not incorporated wind power uncertainty into the entire optimization process, still has certain potentials to deal with such issues in practical applications.

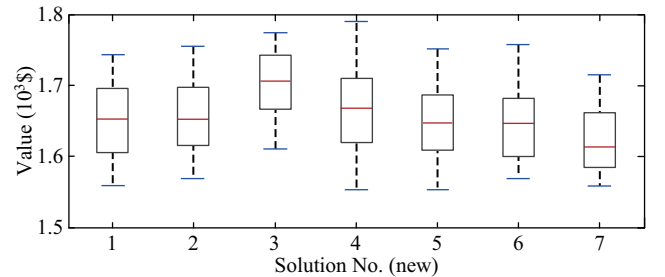


Fig. 11. Box plots for comparison between cost results of individual tests: the red line is the median, the boxes represent the range between the 25th and the 75th quartiles, and the blue lines represent maximum and minimum values.

VI. CONCLUSION AND FUTURE WORK

This paper introduces a novel integrated system, consisting of wind farms, a CCS, and BSSs, to promote both EVs and wind power, and it establishes a joint optimal scheduling model for the proposed W-BSCS. The model comprehensively considers the generation plan of wind power, the charging/discharging scheduling of EV batteries in the W-CCS, the FCB demands and time windows of BSSs, and the VRP of BTs. And it is solved using a heuristic method based on the exhaustive search and the Genetic Algorithm. Case studies demonstrate the effectiveness of the proposed model and show that the W-BSCS can effectively improve the economics of

the integrated system, reduce wind curtailment, and address environmental concerns of deploying large scale EVs.

This study contributes to the integrated development of the power system and the transportation system. In a future study, we will focus on developing some exact solution methods for the proposed problem, and two-stage or multi-stage stochastic programming will be employed to enhance the effectiveness of the proposed model in practical applications.

REFERENCES

- [1] International Energy Agency. (2018). *Global EV Outlook 2018*. [Online]. Available: <https://webstore.iea.org/global-ev-outlook-2018>.
- [2] S. Shafiee, M. Fotuhi-Firuzabad, and M. Rastegar, "Investigating the impacts of plug-in hybrid electric vehicles on power distribution systems," *IEEE Transactions on Smart Grid*, vol. 4, no. 3, pp. 1351–1360, Sep. 2013.
- [3] J. Tomić and W. Kempton, "Using fleets of electric-drive vehicles for grid support," *Journal of Power Sources*, vol. 168, no. 2, pp. 459–468, Jun. 2007.
- [4] M. S. Islam, N. Mithulananthan, and K. Y. Lee, "Suitability of PV and battery storage in EV charging at business premises," *IEEE Transactions on Power Systems*, vol. 33, no. 4, pp. 4382–4396, Jul. 2018.
- [5] M. D. Galus, R. A. Waraich, F. Noembrini, K. Steurs, G. Georges, K. Boulouchos, K. W. Axhausen, and G. Andersson, "Integrating power systems, transport systems and vehicle technology for electric mobility impact assessment and efficient control," *IEEE Transactions on Smart Grid*, vol. 3, no. 2, pp. 934–949, Jun. 2012.
- [6] E. X. Yao, V. W. S. Wong, and R. Schober, "Optimization of aggregate capacity of PEVs for frequency regulation service in day-ahead market," *IEEE Transactions on Smart Grid*, vol. 9, no. 4, pp. 3519–3529, Jul. 2018.
- [7] H. Liu, J. J. Qi, J. H. Wang, P. J. Li, C. B. Li, and H. Wei, "EV dispatch control for supplementary frequency regulation considering the expectation of EV owners," *IEEE Transactions on Smart Grid*, vol. 9, no. 4, pp. 3763–3772, Jul. 2018.
- [8] T. Y. Zhao, Y. Z. Li, X. W. Pan, P. Wang, and J. H. Zhang, "Real-time optimal energy and reserve management of electric vehicle fast charging station: hierarchical game approach," *IEEE Transactions on Smart Grid*, vol. 9, no. 5, pp. 5357–5370, Sep. 2018.
- [9] J. Zhao, C. Wan, Z. Xu, and K. P. Wong, "Spinning reserve requirement optimization considering integration of plug-in electric vehicles," *IEEE Transactions on Smart Grid*, vol. 8, no. 4, pp. 2009–2021, Jul. 2017.
- [10] M. Alizadeh, H. T. Wai, M. Chowdhury, A. Goldsmith, A. Scaglione, and T. Javidi, "Optimal pricing to manage electric vehicles in coupled power and transportation networks," *IEEE Transactions on Control of Network Systems*, vol. 4, no. 4, pp. 863–875, Dec. 2017.
- [11] Q. L. Huang, Q. S. Jia, and X. H. Guan, "Robust scheduling of EV charging load with uncertain wind power integration," *IEEE Transactions on Smart Grid*, vol. 9, no. 2, pp. 1043–1054, Mar. 2018.
- [12] A. Kavousi-Fard, T. Niknam, and M. Fotuhi-Firuzabad, "Stochastic re-configuration and optimal coordination of V2G plug-in electric vehicles considering correlated wind power generation," *IEEE Transactions on Sustainable Energy*, vol. 6, no. 3, pp. 822–830, Jul. 2015.
- [13] W. F. Zhong, R. Yu, S. L. Xie, Y. Zhang, and D. K. Y. Yau, "On stability and robustness of demand response in V2G mobile energy networks," *IEEE Transactions on Smart Grid*, vol. 9, no. 4, pp. 3203–3212, Jul. 2018.
- [14] M. E. Khodayar, L. Wu, and M. Shahidehpour, "Hourly coordination of electric vehicle operation and volatile wind power generation in SCUC," *IEEE Transactions on Smart Grid*, vol. 3, no. 3, pp. 1271–1279, Sep. 2012.
- [15] S. H. Yao, P. Wang, X. C. Liu, H. J. Zhang, and T. Y. Zhao, "Rolling Optimization of Mobile Energy Storage Fleets for Resilient Service Restoration," *IEEE Transactions on Smart Grid*, vol. 11, no. 2, pp. 1030–1043, Mar. 2020.
- [16] M. Wang, M. Ismail, R. Zhang, X. M. Shen, E. Serpedin, and K. Qaraqe, "Spatio-temporal coordinated V2V energy swapping strategy for mobile PEVs," *IEEE Transactions on Smart Grid*, vol. 9, no. 3, pp. 1566–1579, May 2018.
- [17] G. Wenzel, M. Negrete-Pincetic, D. E. Olivares, J. MacDonald, and D. S. Callaway, "Real-time charging strategies for an electric vehicle aggregator to provide ancillary services," *IEEE Transactions on Smart Grid*, vol. 9, no. 5, pp. 5141–5151, Sep. 2018.
- [18] A. Weis, J. J. Michalek, P. Jaramillo, and R. Lueken, "Emissions and cost implications of controlled electric vehicle charging in the U.S. PJM interconnection," *Environmental Science & Technology*, vol. 49, no. 9, pp. 5813–5819, Apr. 2015.
- [19] M. A. M. Tamayao, J. J. Michalek, C. Hendrickson, and I. M. L. Azevedo, "Regional variability and uncertainty of electric vehicle life cycle CO₂ emissions across the United States," *Environmental Science & Technology*, vol. 49, no. 14, pp. 8844–8855, Jun. 2015.
- [20] Y. Li, C. Davis, Z. Lukszo, and M. Weijnen, "Electric vehicle charging in China's power system: energy, economic and environmental trade-offs and policy implications," *Applied Energy*, vol. 173, pp. 535–554, Jul. 2016.
- [21] W. Tushar, C. Yuen, S. S. Huang, D. B. Smith, and H. V. Poor, "Cost minimization of charging stations with photovoltaics: an approach with EV classification," *IEEE Transactions on Intelligent Transportation Systems*, vol. 17, no. 1, pp. 156–169, Jan. 2016.
- [22] H. M. Chung, W. T. Li, C. Yuen, C. K. Wen, and N. Crespi, "Electric vehicle charge scheduling mechanism to maximize cost efficiency and user convenience," *IEEE Transactions on Smart Grid*, vol. 10, no. 3, pp. 3020–3030, May 2019.
- [23] X. M. Wang, C. Yuen, N. U. Hassan, N. An, and W. W. Wu, "Electric vehicle charging station placement for urban public bus systems," *IEEE Transactions on Intelligent Transportation Systems*, vol. 18, no. 1, pp. 128–139, Jan. 2017.
- [24] P. C. You, Z. Y. Yang, Y. M. Zhang, S. H. Low, and Y. X. Sun, "Optimal charging schedule for a battery switching station serving electric buses," *IEEE Transactions on Power Systems*, vol. 31, no. 5, pp. 3473–3483, Sep. 2016.
- [25] B. Sun, X. Q. Tan, and D. H. K. Tsang, "Optimal charging operation of battery swapping and charging stations with QoS guarantee," *IEEE Transactions on Smart Grid*, vol. 9, no. 5, pp. 4689–4701, Sep. 2018.
- [26] M. R. Sarker, H. Pandžić, and M. A. Ortega-Vazquez, "Optimal operation and services scheduling for an electric vehicle battery swapping station," *IEEE Transactions on Power Systems*, vol. 30, no. 2, pp. 901–910, Mar. 2015.
- [27] X. Q. Tan, G. N. Qu, B. Sun, N. Li, and D. H. K. Tsang, "Optimal scheduling of battery charging station serving electric vehicles based on battery swapping," *IEEE Transactions on Smart Grid*, vol. 10, no. 2, pp. 1372–1384, Mar. 2019.
- [28] M. Takagi, Y. Iwafune, K. Yamaji, H. Yamamoto, K. Okano, P. Hiwatari, and T. Ikeya, "Economic value of PV energy storage using batteries of battery-switch stations," *IEEE Transactions on Sustainable Energy*, vol. 4, no. 1, pp. 164–173, Jan. 2013.
- [29] A. Jhunjhunwala, P. Kaur, and S. Mutagekar, "Electric vehicles in India: a novel approach to scale electrification," *IEEE Electrification Magazine*, vol. 6, no. 4, pp. 40–47, Dec. 2018.
- [30] P. C. You, S. H. Low, W. Tushar, G. C. Geng, C. Yuen, Z. Y. Yang, and Y. X. Sun, "Scheduling of EV battery swapping—part I: centralized solution," *IEEE Transactions on Control of Network Systems*, vol. 5, no. 4, pp. 1887–1897, Dec. 2018.
- [31] P. C. You, S. H. Low, L. Zhang, R. L. Deng, G. B. Giannakis, Y. X. Sun, and Z. Y. Yang, "Scheduling of EV battery swapping—Part II: distributed solutions," *IEEE Transactions on Control of Network Systems*, vol. 5, no. 4, pp. 1920–1930, Dec. 2018.
- [32] H. Y. Mak, Y. Rong, and Z. J. M. Shen, "Infrastructure planning for electric vehicles with battery swapping," *Management Science*, vol. 59, no. 7, pp. 1479–1724, Jul. 2013.
- [33] R. Rao, X. P. Zhang, J. Xie, and L. W. Ju, "Optimizing electric vehicle users' charging behavior in battery swapping mode," *Applied Energy*, vol. 155, pp. 547–559, Oct. 2015.
- [34] X. C. Liu, T. Y. Zhao, S. H. Yao, C. B. Soh, and P. Wang, "Distributed operation management of battery swapping-charging systems," *IEEE Transactions on Smart Grid*, vol. 10, no. 5, pp. 5320–5333, Sep. 2019.
- [35] Y. Zheng, Z. Y. Dong, Y. Xu, K. Meng, J. H. Zhao, and J. Qiu, "Electric vehicle battery charging/swap stations in distribution systems: comparison study and optimal planning," *IEEE Transactions on Power Systems*, vol. 29, no. 1, pp. 221–229, Jan. 2014.
- [36] T. Y. Zhao, J. H. Zhang, P. Wang, "Quality-of-service closed-loop supply chain based battery swapping and charging system operation: A hierarchy game approach," *CSEE Journal of Power and Energy Systems*, vol. 5, no. 1, pp. 35–45, Jan. 2019.
- [37] M. F. Ban, J. L. Yu, Z. Y. Li, D. Y. Guo, and J. Ge, "Battery swapping: An aggressive approach to transportation electrification," *IEEE Electrification Magazine*, vol. 7, no. 3, pp. 44–54, Sep. 2019.
- [38] Z. X. Liu, Q. W. Wu, S. J. Huang, L. F. Wang, M. Shahidehpour, and Y. S. Xue, "Optimal day-ahead charging scheduling of electric vehicles

- through an aggregative game model," *IEEE Transactions on Smart Grid*, vol. 9, no. 5, pp. 5173–5184, Sep. 2018.
- [39] T. Y. Zhang, X. Chen, Z. Yu, X. Y. Zhu, and D. Shi, "A monte carlo simulation approach to evaluate service capacities of EV charging and battery swapping stations," *IEEE Transactions on Industrial Informatics*, vol. 14, no. 9, pp. 3914–3923, Sep. 2018.
- [40] Y. N. Liang and X. P. Zhang, "Battery swap pricing and charging strategy for electric taxis in China," *Energy*, vol. 147, pp. 561–577, Mar. 2018.
- [41] T. Long, Z. H. Bie, L. Z. Jiang, H. P. Xie, "Coordinated dispatch of integrated electricity-natural gas system and the freight railway network," *CSEE Journal of Power and Energy Systems*, vol. 6, no. 4, pp. 782–792, Sep. 2020.
- [42] Y. Zhang, J. H. Yuan, C. H. Zhao, and L. Q. Lyu, "Can dispersed wind power take off in China: a technical & institutional economics analysis," *Journal of Cleaner Production*, vol. 256, pp. 120475, May 2020.
- [43] W. Tushar, B. Chai, C. Yuen, S. S. Huang, D. B. Smith, H. V. Poor, and Z. Y. Yang, "Energy storage sharing in smart grid: a modified auction-based approach," *IEEE Transactions on Smart Grid*, vol. 7, no. 3, pp. 1462–1475, May 2016.
- [44] W. Tushar, C. Yuen, H. Mohsenian-Rad, T. Saha, H. V. Poor, and K. L. Wood, "Transforming energy networks via peer-to-peer energy trading: the potential of game-theoretic approaches," *IEEE Signal Processing Magazine*, vol. 35, no. 4, pp. 90–111, Jul. 2018.
- [45] A. V. Savkin, M. Khalid, and V. G. Agelidis, "A constrained monotonic charging/discharging strategy for optimal capacity of battery energy storage supporting wind farms," *IEEE Transactions on Sustainable Energy*, vol. 7, no. 3, pp.1224–1231, Jul. 2016.
- [46] Z. Y. Li, M. Shahidehpour, S. Bahramirad, and A. Khodaei, "Optimizing traffic signal settings in smart cities," *IEEE Transactions on Smart Grid*, vol. 8, no. 5, pp. 2382–2393, Sep. 2017.
- [47] H. Miao, G. Chen, C. J. Li, Z. Y. Dong, and K. P. Wong, "Operating expense optimization for EVs in multiple depots and charge stations environment using evolutionary heuristic method," *IEEE Transactions on Smart Grid*, vol. 9, no. 6, pp. 6599–6611, Nov. 2018.
- [48] M. F. Ban, J. L. Yu, M. Shahidehpour, and Y. Y. Yao, "Integration of power-to-hydrogen in day-ahead security-constrained unit commitment with high wind penetration," *Journal of Modern Power Systems and Clean Energy*, vol. 5, no. 3, pp. 337–349, Apr. 2017.
- [49] N. T. Huang, W. T. Wang, and G. W. Cai, "Optimal configuration planning of multi-energy microgrid based on deep joint generation of source-load-temperature scenarios," in *CSEE Journal of Power and Energy Systems*, doi: 10.17775/CSEEPES.2020.01090.



Mingfei Ban received the B.S., M.S. and Ph.D. degrees in Electrical Engineering at Harbin Institute of Technology (HIT), Harbin, China, in 2011, 2013, and 2019 respectively. He was a visiting Ph.D. student at Illinois Institute of Technology. He is currently an Associate Professor with the College of Mechanical and Electrical Engineering, Northeast Forestry University, China. His research interests include sustainable energy, electrical vehicles, and microgrids.



Jilai Yu received the B.S. and M.S. degrees in Harbin Institute of Technology (HIT), Harbin, China, in 1988 and 1990, respectively, and the Ph.D. degree in North China Institute of Electric Power, Baoding, China, in 1992. As a postdoctoral researcher, he joined the Department of Electrical Engineering of HIT in 1992. He was an Associate Professor in the Department of Electrical Engineering of HIT in 1994. He has been a professor in the Department of Electrical Engineering of HIT since 1998. His current research interests include power

system analysis and control, optimal dispatch of power system, green power and smart grid.



Yiyun Yao received the B.S. degree from Chongqing University, China, in 2012, M.S. degree and Ph.D. degree from the Illinois Institute of Technology (IIT), Chicago, in 2015 and 2019, all in Electrical Engineering. He is currently working at National Renewable Energy Laboratory. His research interests include operation, security and economics of electric power systems.